

1 **Large upper tropospheric ozone enhancements above mid-latitude**
2 **North America during summer: In situ evidence from the IONS and**
3 **MOZAIC ozone measurement network**

4

5 O. R. Cooper^{1,2}, A. Stohl³, M. Trainer², A. M. Thompson⁴, J. C. Witte⁵, S. J. Oltmans², G.
6 Morris⁶, K. E. Pickering⁷, J. H. Crawford⁸, Gao Chen⁸, R. C. Cohen⁹, T. H. Bertram⁹, P.
7 Wooldridge⁹, A. Perring⁹, W. H. Brune⁴, J. Merrill¹⁰, J. L. Moody¹¹, D. Tarasick¹², P. Nédélec¹³,
8 G. Forbes¹⁴, M. J. Newchurch¹⁵, F. J. Schmidlin¹⁶, B. J. Johnson², S. Turquety¹⁷, S. L.
9 Baughcum¹⁸, X. Ren⁴, F. C. Fehsenfeld², J. F. Meagher², N. Spichtinger¹⁹, C. C. Brown⁸, S. A.
10 McKeen^{1,2}, I. S. McDermid²⁰, and T. Leblanc²⁰

11

12

13 ¹Cooperative Institute for Research in Environmental Sciences, University of Colorado, Boulder, USA

14 ²NOAA Earth System Research Laboratory, Boulder, USA

15 ³Norwegian Institute for Air Research, Kjeller, Norway

16 ⁴Department of Meteorology, Pennsylvania State University, University Park, USA

17 ⁵Science Systems and Applications, Inc., NASA Goddard Space Flight Center, Greenbelt, USA

18 ⁶Department of Physics & Astronomy, Valparaiso University, Valparaiso, Indiana, USA

19 ⁷Laboratory for Atmospheres, NASA Goddard Space Flight Center, Greenbelt, MD USA

20 ⁸NASA Langley Research Center, Hampton, USA

21 ⁹Department of Chemistry and Department of Earth and Planetary Science, University of California,
22 Berkeley

23 ¹⁰Graduate School of Oceanography, University of Rhode Island, Narragansett, USA

24 ¹¹Department of Environmental Sciences, University of Virginia, Charlottesville, USA

25 ¹²Experimental Studies Research Division, MSC/Environment Canada, Downsview, Canada

26 ¹³Laboratoire d'Aerologie - CNRS – OMP, Toulouse, France

1 ¹⁴Meteorological Service of Canada, Sable Island, Nova Scotia, Canada

2 ¹⁵Atmospheric Science Department, University of Alabama in Huntsville, USA

3 ¹⁶NASA/GSFC/Wallops Flight Facility, Wallops Island, Virginia, USA

4 ¹⁷Atmospheric Chemistry Modeling Group, Division of Engineering and Applied Sciences, Harvard
5 University, Cambridge, USA

6 ¹⁸Boeing Company, Seattle, USA

7 ¹⁹Department of Ecology, Technical University of Munich

8 ²⁰Table Mountain Facility, Jet Propulsion Laboratory, California Institute of Technology, Wrightwood

9

10 **Submitted to JGR-Atmospheres March 16, 2006**

11 **Revised June 14, 2006**

12

13 **Contact information:**

14 Owen R. Cooper

15 Cooperative Institute for Research in Environmental Sciences (CIRES)

16 NOAA Earth System Research Laboratory

17 Chemical Sciences Division, Theoretical Aeronomy Branch

18 CSD04

19 325 Broadway

20 Boulder CO 80305

21 ph: (303) 497-3599

22 E-mail: Owen.R.Cooper@noaa.gov

1 **Abstract.**

2 The most extensive set of free tropospheric ozone measurements ever compiled across
3 mid-latitude North America was measured with daily ozonesondes, commercial aircraft and a
4 lidar at 14 sites during July-August 2004. The model estimated stratospheric ozone was
5 subtracted from all profiles, leaving a tropospheric ozone residual. On average the upper
6 troposphere above mid-latitude eastern North America contained 15 ppbv more tropospheric
7 residual ozone than the more polluted layer between the surface and 2 km above sea level.
8 Lowest ozone values in the upper troposphere were found above the two upwind sites in
9 California. The upper troposphere above mid-latitude eastern North America contained 16 ppbv
10 more tropospheric residual ozone than the upper troposphere above 3 upwind sites, with the
11 greatest enhancement above Houston, Texas at 24 ppbv. Upper tropospheric CO measurements
12 above east Texas show no statistically significant enhancement compared to west coast
13 measurements, arguing against a strong influence from fresh surface anthropogenic emissions to
14 the upper troposphere above Texas where the ozone enhancement is greatest. Vertical mixing of
15 ozone from the boundary layer to the upper troposphere can only account for 2 ppbv of the 16
16 ppbv ozone enhancement above eastern North America, therefore the remaining 14 ppbv must be
17 the result of in situ ozone production. The transport of NO_x tracers from North American
18 anthropogenic, biogenic, biomass burning, and lightning emissions was simulated for the upper
19 troposphere of North America with a particle dispersion model. Additional box model
20 calculations suggest the 24 ppbv ozone enhancement above Houston can be produced over a ten
21 day period from oxidation reactions of lightning NO_x and background mixing ratios of CO and
22 CH₄. Overall, we estimate that 69-84% (11-13 ppbv) of the 16 ppbv ozone enhancement above
23 eastern North America is due to in situ ozone production from lightning NO_x with the remainder
24 due to transport of ozone from the surface or in situ ozone production from other sources of NO_x.

1 **1. Introduction**

2 Ozone is a key trace gas for both the chemistry and radiative balance of the troposphere
3 [IPCC, 2001], and as it is the principal pollutant associated with photochemical smog its presence
4 in the lower troposphere has large implications for issues of air quality. Currently, international
5 research programs such as the SPARC Project (Stratospheric Processes and their Role in Climate)
6 and IGAC (International Global Atmospheric Chemistry) are focusing research on the dynamics
7 and composition of the upper troposphere and lower stratosphere because of this region's
8 influence on global climate change, with ozone once again a trace gas of primary interest.

9 Chemical transport model (CTM) studies indicate that North American emissions have a
10 major impact on net global tropospheric ozone production [Li *et al.*, 2002]. However, verifying
11 CTM estimates of the North American ozone budget is difficult due to the limited number of
12 profiling sites across the continent. Long-term ozonesonde profiling has been conducted at six
13 locations in Canada, but all are at relatively high latitudes [Tarasick *et al.*, 2005], and at just two
14 sites in the USA: Boulder, Colorado and Wallops Island, Virginia. However, the National
15 Oceanic and Atmospheric Administration (NOAA) initiated the Trinidad Head, California and
16 Huntsville, Alabama sites in the late 1990's [Newchurch *et al.*, 2003]. Data coverage increased in
17 2004 with the addition of the NOAA site at Narragansett, Rhode Island, and four new Canadian
18 sites along the USA/Canada border. However, large data gaps still exist in the southwestern and
19 south-central USA and the sampling rate of once per week means it will take several years to
20 build a North American ozone climatology.

21 To finally measure the daily ozone distribution across mid-latitude North America during
22 the most photochemically active part of the year, NASA, NOAA, Environment Canada, and
23 several US universities pooled resources during the July 1 – August 15, 2004, ICARTT
24 (International Consortium for Atmospheric Research on Transport and Transformation) study to
25 launch ozonesondes from several sites across the eastern USA and Canada under the IONS
26 (INTEX Ozonesonde Network Study) program [see overview of IONS by Thompson *et al.*,

1 2006]. Additional ozone profiles across eastern North America were obtained from five
2 instrumented commercial aircraft that fly between North America and Europe under the European
3 MOZAIC program. To increase the sample size, MOZAIC profiles were combined with
4 ozonesonde profiles from nearby locations to form 13 free-tropospheric ozone measurement sites
5 (Figures 1 and 3a). An additional upper tropospheric ozone monitoring site was available near
6 Los Angeles from combined lidar and MOZAIC measurements. This dataset contains the most
7 extensive set of free tropospheric ozone measurements ever compiled across mid-latitude North
8 America. In this study we focus on measurements that were made only in the troposphere and
9 subtract the model-estimated stratospheric ozone from each profile leaving a tropospheric ozone
10 residual. An interesting result was that the overall network showed a greater amount of
11 tropospheric residual ozone in the upper troposphere than in the lower troposphere. Furthermore
12 the upper troposphere above eastern North America contained far greater tropospheric residual
13 ozone mixing ratios than the upwind sites, with the largest values above Houston, Texas. We use
14 a particle dispersion model to demonstrate that the upper tropospheric ozone maximum above
15 eastern North America is largely the result of in situ ozone production from lightning NO_x.

16 **2. Method**

17 **2.1 Trace gas measurements**

18 This study utilizes 260 ozone profiles measured by balloon-borne ozonesondes equipped
19 with electrochemical concentration cell sensors that have an accuracy of about 10% in the
20 troposphere, except when ozone is less than 10 ppbv when accuracies can be degraded to 15%
21 [Newchurch *et al.*, 2003]. Another 183 ozone profiles were measured by five MOZAIC
22 commercial aircraft using a dual-beam UV absorption instrument (Thermo-Electron, model 49-
23 103), with an estimated accuracy of $\pm (2 \text{ ppbv} + 2\%)$ [Thouret *et al.*, 1998]. Sites containing only
24 MOZAIC measurements are New York City, Montreal and Atlanta. Sites containing a
25 combination of MOZAIC and nearby ozonesonde profiles are Houston, Ontario and Washington

1 DC. All other sites contain only ozonesonde measurements. For this study all individual ozone
2 profiles were smoothed in the vertical to 500 m layer averages.

3 The same five MOZAIC aircraft that measure ozone also measure CO using an infrared
4 carbon monoxide analyzer with a performance suitable for routine aircraft measurements: ± 5
5 ppbv, $\pm 5\%$ precision for a 30 s response time [Nedelec *et al.*, 2003].

6 The NASA Jet Propulsion Laboratory (JPL) operates two differential absorption ozone
7 lidars at the Table Mountain Facility northeast of Los Angeles to cover the altitude range 4-55 km
8 [McDermid *et al.*, 2002]. The ozone profiles used in this study (4-27 km) were retrieved using a
9 combination of all the channels of the tropospheric system and one channel of the stratospheric
10 system. For a typical 2-hour integrated nighttime profile the system is accurate to within 5% -
11 25% (0.05 to 0.3×10^{12} molecules/cm³), with the largest deviations occurring when the free
12 tropospheric ozone mixing ratios are very low.

13 Nitrogen Dioxide (NO₂) mixing ratios were measured directly aboard the NASA DC-8 by
14 Laser Induced Fluorescence (LIF) [Thornton *et al.* 2000; Bertram *et al.* 2006] on all 18 flights
15 during ICARTT above North America and the western North Atlantic Ocean. Briefly, NO₂ is
16 excited at 585 nm using a Nd:YAG pumped tunable dye laser and the resulting red-shifted
17 fluorescence is imaged onto a photomultiplier tube following optical and temporal filtering. A
18 supersonic expansion is used in the detection region to increase the population of NO₂ in the
19 excited rotational state, leading to a factor-of-thirty enhancement in signal [Cleary *et al.*, 2002].
20 The detection sensitivity of this instrument is 0.8ppt/min at S/N=2. The uncertainty in the
21 instrument zero is less than 1ppt.

22 NO was measured directly aboard the NASA DC-8 by a commercial NO-NO_x analyzer
23 (Model TEI 42C) based on the chemiluminescence technique. The instrument was run in NO
24 single mode only, and an in-situ NO calibration system was used for frequent NO span and
25 background checks. The detection limit of this instrument is about 50 pptv with 1 minute
26 integration time.

1 A whole air sampler on board the DC-8 collected air samples in electro-polished stainless
2 steel canisters every few minutes during each flight. The canisters were shipped to the University
3 of California, Irvine for analysis. An HP6890 gas chromatogram analyzer with a flame-ionization
4 detector was used to measure *i*-pentane and other hydrocarbons [Colman *et al.*, 2001]. Absolute
5 accuracy was better than 10% at 1σ , with a precision of 3%.

6 Throughout this manuscript the ozone and CO distributions are compared between sites
7 at 500 m intervals between the surface and the tropopause. We use the Kruskal-Wallace
8 nonparametric one-way analysis of variance test to determine if the trace gas distributions
9 between two given sites have statistically significant differences at the 95% confidence interval.

10 **2.2 FLEXPART simulations**

11 The global transport and dispersion of North American NO_x emissions from biomass
12 burning, biogenic, lightning, aircraft and surface anthropogenic sources was simulated with the
13 FLEXPART Lagrangian particle dispersion model [Stohl *et al.*, 1998; Stohl *et al.*, 2005], which
14 calculates the trajectories of a multitude of particles. The model was driven by ECMWF wind
15 fields with a temporal resolution of 3 hours (analyses at 0, 6, 12, 18 UTC; 3 hr forecasts at 3, 9,
16 15, 21 UTC), horizontal resolution of 1° x 1°, and 60 vertical levels. Nested ECMWF windfields
17 of 0.36° resolution were used for the area between 108° W - 18° E and 18° - 72° N covering the
18 major anthropogenic and lightning emission regions of North America. Both data sets have 16
19 model layers below 2 km, with 10 layers below 700 m. These data sets approximately represent
20 the full spectral resolution of the ECMWF model at that time. Particles are transported both by
21 the resolved winds and parameterized sub-grid motions. To account for convection, FLEXPART
22 uses the parameterization scheme of Emanuel and Živković-Rothman [1999], which is
23 implemented at each 15-minute model time step, and is intended to describe all types of
24 convection, including the deep convection related to the lightning over the Gulf of Mexico. The
25 scheme was tested by Forster *et al.* [2006] and found to produce convective precipitation
26 amounts that are in relatively good agreement with observations both in the tropics and

1 extratropics, reducing the positive tropical bias of the on-line convection scheme used at
2 ECMWF. It also improves the agreement of FLEXPART simulations with airborne tracer
3 measurements compared to simulations without the convection parameterization.

4 FLEXPART is used to simulate the transport of NO_x emissions from biomass burning,
5 biogenic, lightning, aircraft and surface anthropogenic sources. In this study the tracers are run in
6 forward mode as passive tracers that are not removed by wet or dry deposition processes, neither
7 are the NO_x tracers converted to oxidized species. The tracers are tracked for a variety of time
8 periods including 1, 2, 5 10 and 20 days since emission. For example a lightning NO_x tracer that
9 is tracked for 10 days is referred to as a 10-day lightning NO_x tracer. To simulate the oxidation of
10 NO_x in the upper troposphere a 2-day e-folding lifetime (as determined from box model analysis)
11 is separately applied to all tracers.

12 The stratospheric ozone contribution to each profile was estimated using the FLEXPART
13 retroplume technique [Stohl *et al.*, 2003], as described by Cooper *et al.* [2005a]. Briefly, 40,000
14 back trajectory particles were released from each 500 m layer of each ozone profile. The number
15 of particles that entered the stratosphere over the previous 20 days was tabulated along with their
16 potential vorticity (PV) values. The mass of each particle was scaled by the O₃/PV ratio of the
17 lower stratosphere, as determined from the IONS ozonesondes and ECMWF analyses from the
18 ICARTT study period, to estimate the amount of stratospheric ozone carried by each particle. To
19 account for the fact that the PV value for a given particle changes over time this calculation was
20 performed for each day of the 20-day transport time, with the average calculated ozone value over
21 20 days considered representative of the particle. This calculation also accounted for the fact that
22 the O₃/PV ratio decreases throughout the summer due to the seasonal decrease of ozone in the
23 lowermost stratosphere. These values were integrated over all 40,000 particles in a given
24 retroplume to yield the quantity of stratospheric ozone influencing a particular 500 m layer of an
25 ozone profile. To verify the modeled results, the ratio of modeled/measured ozone values was
26 calculated for all IONS ozonesonde profiles for each 500 m layer in the stratosphere (PV >2).

1 The geometric mean of all the point-by-point ratios of modeled/measured ozone was near unity
2 (0.97), indicating little overall bias in the model. The standard error of the modeled stratospheric
3 ozone compared to measured ozone was a factor of 1.5.

4 **2.3 Lightning NO_x emissions**

5 The lightning NO_x emissions in this study are not produced by a grid-scale model
6 parameterization scheme. Instead, lightning NO_x production was simulated with FLEXPART
7 above North America and the surrounding waters according to the exact times and locations of
8 each cloud-to-ground (CG) lightning flash observed by lightning detection networks. CG flashes
9 were detected over the continental USA by the National Lightning Detection Network (NLDN),
10 with a detection efficiency (DE) better than 90% [Grogan, 2004]. For regions between 21° and
11 60° N, but outside of the continental USA, CG flashes were detected with the experimental long-
12 range lightning detection network (LRLDN). DE is 60-80% at 60° N and 40-60% at 21° N and
13 increases with proximity to the USA (personal communication, K. Cummins, Vaisala-
14 Thunderstorm). For regions south of 21° N CG and IC flashes were quantified according to a
15 seasonally and diurnally varying climatology based on five years of data from the polar orbiting
16 Lightning Imaging Sensor (LIS) and Optical Transient Detector (OTD) instruments [Christian *et*
17 *al.*, 2003].

18 To account for the drop-off in detection efficiency south of the USA all NO_x emissions
19 from LRLDN flashes in this region were scaled by the inverse of the DE. Furthermore we scaled
20 the NO_x emissions per CG flash to account for the intra-cloud (IC) flashes not detected by the
21 NLDN and LRLDN. Monthly gridded IC:CG ratios calculated for the continental United States
22 were applied to the NLDN data [Bocippio *et al.*, 2001]. Monthly mean IC:CG values typically
23 range between 1 and 10 for individual 0.5°x0.5° grid cells, with an average value of 4.2 above the
24 continental USA during the study period of June 21 through August 15. This average value of
25 4.2 was applied to the LRLDN data

1 We selected a lightning NO_x emission rate of 6.4 kg N flash⁻¹ based on the analysis of
2 North American thunderstorms by *DeCaria et al.* [2005]. Between June 21 and August 15, 2004,
3 a single FLEXPART trajectory particle was released at the exact time and location of the 32
4 million CG lightning flashes detected by the NLDN and LRLDN. Another 15 million trajectory
5 particles were released from the region of the lightning climatology (representing 30 million IC
6 and CG flashes). Computer memory limitations only permitted the release of one FLEXPART
7 particle per flash. To account for the fact that lightning NO_x emissions occur mainly in the upper
8 troposphere but over a wide range of altitudes [*Pickering et al.*, 1998; *DeCaria et al.*, 2005], the
9 particles were released between the tropopause and 6 km above sea level according to a normal
10 distribution which was allowed to slide up and down with the height of the tropopause. No
11 particles were released below 6 km and the mode of the release height was between 10 and 11
12 km. Upon release the particles were permitted to move vertically according to the model vertical
13 winds and the convection scheme.

14 The distribution of the lightning N emissions is shown in Figure 2. The major regions for
15 lightning emissions are located 1) along the Sierra Madre Mountains of northwestern Mexico, 2)
16 above Cuba, and 3) a band stretching along the northern coast of the Gulf of Mexico, extending
17 across Florida and into the westernmost North Atlantic Ocean off the southeastern USA.
18 Lightning is also prevalent across the USA, east of the Rocky Mountains. These lightning regions
19 generally correspond to the most intense regions of lightning depicted by lightning climatologies
20 [*Christian et al.*, 2003; *Orville et al.*, 2002]. The exception is that the lightning along the
21 northern coast of the Gulf of Mexico extends further south than shown by *Christian et al.* [2003],
22 and the lightning is relatively more intense off the coast of the southeastern USA than shown by
23 *Christian et al.* [2003]. These lightning regions correspond to precipitation maxima above the
24 northern Gulf coast and the westernmost North Atlantic Ocean during summer 2004 (as shown in
25 monthly precipitation plots produced by the Global Precipitation Climatology Project (GPCP))
26 and are the result of several cold fronts that pushed off shore during the study period. The

1 lightning emissions south of 21° N are tied to the lightning climatology of *Christian et al.* [2003]
2 and appear very diffuse in comparison to the NLDN and LRLDN lightning emissions due to
3 heavy smoothing over 2.5°x2.5° grid cells and boxcar smoothing across several weeks.

4 Multiplying our lightning NO_x emission rate by the global lightning flash rate of 44
5 flashes second⁻¹ as determined from satellite observations [*Christian et al.*, 2003] yields a global
6 lightning NO_x production of 8.9 Tg N year⁻¹. The 47 million FLEXPART particles in the
7 simulation represent the transport of 1.2 Tg of lightning N from 194 million IC and CG flashes
8 over the study region between June 21 and August 15, 2004. These emissions occur during the
9 peak lightning season in one of the world's most intense lightning regions and represent an
10 estimated 13% of the assumed 8.9 Tg global annual lightning N emissions.

11 **2.4 Other NO_x Emission Inventories**

12 North American emissions were based on the point, on-road, non-road and area sources
13 from the U.S. EPA National Emissions Inventory, base year 1999, with spatial partitioning of
14 area type sources at 4 km resolution. This database covers the USA, Mexican emissions north of
15 24° N, and all Canadian sources south of 52° N [*Frost et al.*, 2005]. Emissions for all other
16 regions of North America and the rest of the northern hemisphere were taken from the EDGAR
17 3.2 Fast Track 2000 dataset, which estimates year 2000 emissions using the EDGAR 3.2
18 estimates for 1995 and trend analyses for the individual countries. EDGAR uncertainty estimates
19 are roughly 50% or greater [*Olivier and Berdowski*, 2001].

20 Biomass burning NO_x tracer was released from a 1° x 1° grid of daily average emissions
21 from forest and peat fires [*Turquety et al.*, 2006]. The emission inventory for North America was
22 generated using MODIS hotspots and reported area burned and information on type of vegetation,
23 fuel loading, and emission factors. Emissions for the rest of the world are based on 2004 monthly
24 MODIS hotspots. The biomass burning NO_x tracer was emitted between the surface and 5000 m
25 as an attempt to account for the uncertain altitude reached by the hot and buoyant boreal smoke
26 plumes.

1 An aircraft NO_x tracer was released in the northern hemisphere using a global emission
2 inventory of aircraft emissions created by combining the civil traffic inventory for 1999 of *Sutkus*
3 *et al.* [2001] with an estimate for 1999 military, charter, and general aviation obtained by
4 extrapolating the earlier inventory work of *Mortlock and van Alstyne* [1998]. Emissions in these
5 inventories were calculated using great circle routes and provided on a 1° x 1° by 1 km altitude
6 grid for each month of 1999. Actual civil aircraft routes vary from day to day because of air
7 traffic congestion, prevailing winds or to avoid turbulence. The use of idealized great circle
8 routes as opposed to actual flight routes can result in some errors but this has been found to be
9 relatively small (~ 5%) [*Forster et al.*, 2003].

10 Soil biogenic NO_x emissions are prescribed according to the Biogenic Emissions
11 Inventory System version 3.11 (BEISv3.11) available through the U.S. EPA
12 (<ftp://ftp.epa.gov/amd/asmd/beis3v11>). These emissions are based on the vegetative dependent
13 emission parameters within BEIS2 (normalized at 30°C) and the 1 km horizontal resolution
14 Biogenic Emissions Landuse Database (BELD) as outlined in *Pierce et al.* [1998]. BEIS3
15 updates to soil NO_x emissions include canopy recapture factors, and day-of-year specific
16 correction factors for growing season and fertilization rates given by *Yienger and Levy* [1995].

17 **2.5 Auxiliary Animation**

18 An auxiliary animation of the FLEXPART lightning NO_x tracer is included with this
19 paper. While the animation is not essential for understanding the results presented here, viewing it
20 allows the reader to clearly see the temporal and spatial evolution of the lightning NO_x tracer.
21 The animation shows the location of a 10-day lightning NO_x tracer expressed as a column value
22 above North America and the North Atlantic Ocean, every two hours between July 1 and August
23 15, 2004. The animation can be viewed at:

24 http://www.al.noaa.gov/metproducts/dc3/images/FLXP_10day_lightning_NOx.mov

25 and requires the Quicktime Player, freely available at <http://www.apple.com/quicktime>.

26 **3. Results**

1 **3.1 The tropospheric ozone distribution across mid-latitude North America**

2 Figure 3a shows the median and standard deviation ozone profiles at the 13 sites that
3 provide full tropospheric and stratospheric measurements during the ICARTT study period.
4 Ozone is much greater in the 6-12 km range than in the lower troposphere and the standard
5 deviation is also generally greater at these altitudes, but much of this influence is due to a
6 stratospheric ozone component. The influence from the stratosphere results from a lower
7 tropopause when a site is north of the polar jet stream and from stratospheric intrusions which are
8 common at mid-latitudes, even in summer [Thompson *et al.*, 2006]. The only site with a low
9 standard deviation in the upper troposphere is Houston which is located south of the summertime
10 range of the polar jet stream.

11 The aim of this study is to focus on purely tropospheric measurements requiring the
12 removal of any recent stratospheric influence. We first removed any part of any individual
13 profile with a PV value greater than 1.0 pvu, which removed the stratospheric influence
14 associated with a low tropopause or fresh stratospheric intrusions (typically less than 2-3 days
15 old). At this point any 500 m layer at any site with less than 10 remaining profiles was dropped
16 from the analysis. The median tropospheric ozone profiles are shown in Figure 3b. Above 4 km
17 the ozone values and standard deviations decrease at all 13 site compared to the profiles in Figure
18 3a.

19 We then subtracted from each individual profile the contribution from the stratosphere as
20 determined by the FLEXPART retroplume technique, removing any influence from aged
21 stratospheric intrusions up to 20 days old. The proportion of stratospheric ozone in the upper
22 troposphere (greater than 8 km altitude and $PV < 1.0$) ranged from an average of 27% at Trinidad
23 Head on the west coast to 13% at Sable Island on the east coast. Trinidad Head was immediately
24 downwind of a region of highly active stratosphere-to-troposphere transport. In contrast Sable
25 Island was not strongly influenced by stratospheric intrusions during summer 2004 due to
26 predominantly southerly transport from the tropical and sub-tropical North Atlantic troposphere.

1 Once the stratospheric influence from the previous 20 days has been removed, the ozone
2 profiles are referred to as tropospheric residual profiles (a quantity which should not be confused
3 with the tropospheric ozone residual that can be calculated from solar backscattered ultraviolet
4 and Total Ozone Mapping Spectrometer data as described by *Fishman and Balok* [1999]). The
5 median and standard deviation tropospheric residual profiles for each site are shown in Figure 3c.
6 The standard deviations of the tropospheric residual ozone profiles in the upper troposphere are
7 greater than the tropospheric profiles in Figure 3b due to errors in the calculation of the
8 stratospheric ozone component; Wallops Island stands out as being particularly noisy due to its
9 small sample size (n=18). *Cooper et al.* [2005b] demonstrated that FLEXPART simulates well
10 the transport and decay of stratospheric intrusions far south of their origin along the polar jet
11 stream, capturing the transport of intrusions from the mid-latitude lower stratosphere to the lower
12 troposphere and the marine boundary of the tropical Pacific Ocean. In that study FLEXPART
13 also performed with little bias but with a standard error of 1.5. Much of this error was due to
14 timing differences between the simulated intrusions and measurements (as much as 12-15 hours),
15 or relatively small displacements of modeled intrusions in the vertical. The rest of the error was
16 due to errors in the wind fields and ozone variability in the lower stratosphere not captured by the
17 average ozone/PV relationship. In the present study FLEXPART also has a standard error of 1.5
18 so the modeled and measured ozone values for a given time and location will differ by an average
19 factor of 1.5. But because the model has been shown to perform with little bias and can resolve
20 decaying intrusions, the average influence of stratospheric intrusions at a given location is
21 expected to be fairly accurate.

22 The tropospheric residual ozone profiles represent the median amount of ozone in the
23 troposphere at a given site with either a tropospheric origin or an aged stratospheric origin greater
24 than 20 days. We assume that any remaining stratospheric ozone older than 20 days is dispersed
25 throughout the mid-latitude troposphere and we neglect any weak latitudinal gradient that may
26 still exist. Below 5 km the tropospheric residual ozone profiles are representative of transport

1 along all of the typical pathways that influence a site. Above 5 km where portions of profiles
2 have been removed due to the presence of a low tropopause or strong stratospheric intrusions the
3 profiles are biased away from air masses with polar origins. This bias increases with altitude with
4 profiles above 10 km representative of air masses with mid-latitude or tropical origins, as
5 expected for tropospheric air masses at these altitudes.

6 An interesting result is that the tropospheric residual ozone profiles show an overall
7 increase of ozone with altitude even though the greatest concentrations of anthropogenic ozone
8 precursors are found near the surface (Figure 3c). When stations are considered individually all
9 have significantly more ozone in the upper troposphere (> 6 km) than in the lower troposphere ($<$
10 2 km). When data from all sites are combined the difference is also statistically significant with a
11 median tropospheric residual ozone value of 61 ppbv in the upper troposphere and 46 ppbv in the
12 lower troposphere. When considering just the 12 eastern North America sites the median
13 tropospheric residual ozone value in the upper troposphere is 62 ppbv, and 47 ppbv in the lower
14 troposphere.

15 The lone western North America site of Trinidad Head has, by far, the lowest
16 tropospheric residual ozone values in the upper troposphere. In comparison, the 12 sites in eastern
17 North America show a broad upper tropospheric ozone enhancement. Houston has the greatest
18 values, otherwise none of remaining eleven eastern sites clearly dominates. In comparison to
19 these combined eleven eastern sites, Houston has significantly more ozone between 7.5 and 11.0
20 km.

21 **3.2 Determining upper tropospheric ozone values upwind of North America**

22 Due to the predominantly westerly transport across mid-latitude North America it is
23 convenient to treat Trinidad Head as an ozone monitoring site with upper tropospheric ozone
24 values typical of the air masses that enter western North America from the North Pacific Ocean
25 and subsequently travel across the continent. Figure 4 shows the difference in median
26 tropospheric residual ozone values between each site in eastern North America and the upwind

1 site of Trinidad Head, and also indicates when the differences are statistically significant. North
2 of 44° N Montreal shows no statistically significant difference in ozone above 6 km, but Sable
3 Island and Pellston have several layers with significantly more ozone. In the northeastern USA,
4 the sites of New York City (NYC), Narragansett and the research vessel *Ronald H. Brown* in the
5 Gulf of Maine have 20-30 ppbv excess ozone at 8-11 km, while Ontario further west shows
6 mainly insignificant enhancements. In general the upper tropospheric ozone enhancements are
7 even greater in the southeastern and southern USA with Houston showing the overall greatest
8 enhancements. Enhancements in the southern USA below 1 km are even greater than the upper
9 tropospheric enhancements, but are not so remarkable as strong summertime ozone production
10 near the surface of the southern USA is well documented [*Fiore et al.*, 1998]. Furthermore, these
11 values are compared to very low ozone mixing ratios at Trinidad Head that are mainly
12 representative of the marine boundary layer and lower troposphere of the Pacific Ocean.

13 This comparison indicates a broad upper tropospheric ozone maximum above eastern
14 North America which increases in magnitude towards the south until it reaches a maximum above
15 Houston. But is Trinidad Head truly representative of the ozone flowing into North America, and
16 is it truly upwind of the eastern North America sites? To explore this question we provide ozone
17 measurements from two additional sites: Table Mountain/MOZAIC and Caracas/eastern
18 Caribbean.

19 The Table Mountain/MOZAIC ozone monitoring site contains a combination of ozone
20 profiles from the JPL Table Mountain tropospheric lidar located 60 km northeast of downtown
21 Los Angeles and a MOZAIC aircraft. During the ICARTT study period the lidar produced 17
22 profiles above 4 km altitude. In the same period a MOZAIC aircraft made 22 flights to and from
23 Los Angeles International Airport, but due to instrument problems only 9 ozone profiles were
24 available in the upper troposphere. These 9 profiles were combined with the 17 lidar profiles and
25 the tropospheric ozone residual was calculated for each 500 m layer.

1 We searched the MOZAIC database for ozone profiles south of the USA to determine the
2 ozone mixing ratios that flow into the southern USA with the North American Monsoon which
3 dominates the transport patterns of the southern USA during July and August. We could only
4 find six profiles south of the USA during the ICARTT study period, however we did find 91
5 flights to and from Caracas, Venezuela during July-August from 1999 to 2004, which we used to
6 construct a multi-year composite ozone profile. The flight tracks of the tropical portions of these
7 flights are shown in Figure 1. Comparing these flight tracks to the column lightning NO_x
8 emissions in Figure 2 it is clear that they pass through the tropical easterlies upwind of the
9 regions strongly influenced by North American lightning. These flights are also upwind of the
10 North American monsoon flow, and therefore provide important information on the background
11 ozone entering the southern USA.

12 Figure 5 compares the median tropospheric ozone residual profiles above Houston to
13 Trinidad Head, Caracas and Table Mtn./MOZAIC. All 500 m layers above 6 km contain
14 significantly more ozone above Houston than above these three upwind sites. For good measure
15 we also include the median ozone profile above Hilo, Hawaii in Figure 5d which is at the upwind
16 end of a transport pathway from Hawaii to Houston, indicating that the upper troposphere of the
17 remote North Pacific Ocean has even less ozone than the three upwind sites on the edge of North
18 America. Figure 6 shows the average location of eleven million trajectory particles released
19 continuously during the study period between the tropopause and 6 km altitude above each
20 upwind sites. Air masses from the upper troposphere above Trinidad Head pass directly through
21 the upper troposphere of the ozone measurement sites in the eastern USA and Canada, with lesser
22 influence above the sites in the southern USA. However the air masses above Table
23 Mountain/Los Angeles have a stronger influence on the upper troposphere above the southern
24 USA. In contrast, the air masses from the eastern Caribbean have more variable transport
25 pathways but in general have a strong influence across the southern Caribbean with weak and
26 diffuse transport into the southern USA

1 Median tropospheric residual ozone values above 6 km at Trinidad Head, Table
2 Mtn./MOZAIC and Caracas are 45 ppbv, 45 ppbv and 49 ppbv respectively. The overall upwind
3 tropospheric residual ozone mixing ratio above 6 km is 46 ppbv. The corresponding value above
4 all 12 sites in eastern North America is 62 ppbv, ranging from 54 ppbv above Montreal to 70
5 ppbv above Houston. Because we have already removed the stratospheric influence the ozone
6 enhancement of roughly 16 ppbv in the upper troposphere above eastern North America can only
7 come from two sources: transport of ozone from the lower troposphere to the upper troposphere
8 or in situ ozone production in the free troposphere. Estimating the influence of lower
9 tropospheric ozone on the upper troposphere is difficult because of its temporal and spatial
10 variability across North America. But let's assume the ozone values from the 12 eastern North
11 America sites, that were predominantly measured in early afternoon or early evening, are broadly
12 representative of North American lower tropospheric ozone during the ICARTT study period.
13 The average tropospheric residual ozone value of the eastern North America lower troposphere (<
14 2 km) is 47 ppbv, only one ppbv greater than the upper tropospheric value of the upwind sites. So
15 no matter how much air is transported from the surface of eastern North America and mixed with
16 the air from the upwind sites as it enters the upper troposphere above eastern North America, on
17 average, the upper tropospheric ozone value can't rise above 47 ppbv due to mixing alone. Even
18 if we are very cautious and assume the median ozone mixing ratio of 59 ppbv in the lower
19 troposphere above Houston is representative of eastern North America and assume all of the
20 eastern North America upper troposphere is exposed to the same amount of vertical mixing as
21 Houston (FLEXPART indicates 15% of the mass of the upper troposphere above Houston
22 originates in the mixed layer over the previous 20 days) upper tropospheric ozone would never
23 exceed 48 ppbv due to mixing alone. Therefore at least 14 ppbv of the 16 ppbv ozone
24 enhancement above eastern North America must be the result of in situ ozone production in the
25 free troposphere.

26 **3.3 The upper troposphere above Houston is not heavily polluted**

1 Now that we have established that in situ ozone production is responsible for the majority
2 of the upper tropospheric ozone enhancement above eastern North America we must determine
3 the relative impact of NO_x emissions from lightning, biomass burning, biogenic, aircraft and
4 surface anthropogenic sources. But first we will focus on the upper troposphere of Houston to
5 illustrate that this region is not heavily influenced by pollution and that the ozone production
6 above this site must be strongly associated with lightning NO_x.

7 In situ evidence that the upper troposphere above Houston and east Texas is not heavily
8 polluted comes from the CO profiles measured by MOZAIC aircraft during the ICARTT study
9 period. Figure 7a compares the CO distributions above Los Angeles to the CO distribution above
10 east Texas (flights to and from Houston and Dallas). Above 5 km there is no statistically
11 significant difference between CO at the two sites. While the lower troposphere of the Los
12 Angeles region is heavily polluted, the emissions do not reach the upper troposphere due to a lack
13 of deep convection above coastal southern California. Therefore the CO above LA is
14 representative of CO emissions upwind of North America. Despite Texas being located in the
15 south central United States the upper troposphere above east Texas is no more polluted than the
16 upper tropospheric background air entering the southwestern USA above Los Angeles. In
17 contrast, the eastern sites of Atlanta and Montreal, and the combined sites of New York
18 City/Boston show significantly more CO in the upper troposphere in comparison to Los Angeles.
19 The excess CO is the result of North American anthropogenic CO emissions that are lofted to the
20 upper troposphere across the eastern half of the continent. Above Montreal, and New York
21 City/Boston there was also an influence from CO emissions from the widespread boreal fires in
22 Alaska and western Canada during the summer of 2004. We also compared the MOZAIC CO
23 profiles above Texas to the 60 MOZAIC CO profiles available at Caracas between 2002 and 2004
24 (not shown) and found no statistically significant difference between the two locations above 5
25 km.

1 Figure 8a shows the average source regions of air in the upper troposphere above
2 Houston as determined by the FLEXPART retroplumes released from the ozone profiles. On
3 average 15% of the upper tropospheric air above Houston passed through the mixed layer during
4 the previous 20 days. Figure 8a shows where the retroplumes from the upper troposphere
5 intercepted the lowest 300 m of the atmosphere. While the retroplumes clearly passed over the
6 high emission regions of Houston and the northern coast of the Gulf of Mexico, most of influence
7 is from the cleaner regions of the Gulf of Mexico, southwestern USA and northern Mexico.
8 Figure 8b shows the location of the upper tropospheric retroplumes in the atmosphere above the 5
9 km level. Most of the influence is from the south-central and southwestern USA, northern Mexico
10 and the Gulf of Mexico, with little influence from the eastern or southeastern USA. This transport
11 analysis appears to explain why the MOZAIC aircraft did not detect high levels of pollution
12 above east Texas in the upper troposphere.

13 **3.4 The dominance of lightning NO_x above eastern North America**

14 As shown in Figure 7 and as will be demonstrated below with the FLEXPART
15 simulations the upper troposphere above Houston has a smaller impact from anthropogenic
16 pollution sources than the ozone profile sites along the east coast, even though it has the greatest
17 ozone enhancements. Therefore the in situ ozone production impacting Houston must have a
18 strong contribution from lightning NO_x, a reasonable assumption given that previous research has
19 established that lightning is the largest global source of NO_x in the upper troposphere (see
20 literature review by *Huntrieser et al.* [1998]). Lightning NO_x emissions are particularly strong
21 above southeastern North America where *Ridley et al.* [2004] described Florida thunderstorms as
22 a faucet of reactive nitrogen to the upper troposphere. Measurements from the NASA DC8
23 aircraft support a strong lightning NO_x source in the upper troposphere during ICARTT. Figure
24 9a shows all of the 10-second average NO_x measurements from the DC-8 above North America
25 between 105° and 64° W during the ICARTT study period. The upper tropospheric mixing ratios
26 are almost as great as the lower tropospheric mixing ratios. Figure 9b shows the DC-8 NO_x

1 measurements vs. *i*-pentane measurements. Both trace gases are emitted from fossil fuel
2 combustion. Below 2 km the two trace gases are correlated, but above 8 km they are not.
3 Because *i*-pentane has a much longer lifetime than NO_x we expect its mixing ratio to increase
4 with respect to NO_x in the upper troposphere. Instead the opposite is observed with the full range
5 of *i*-pentane mixing ratios associated with NO_x mixing ratios greater than 500 pptv, indicating an
6 additional source for NO_x, which is most likely lightning.

7 To quantify the contribution of lightning NO_x to the total amount of NO_x in the upper
8 troposphere of North America we used FLEXPART to simulate the transport of NO_x emissions
9 from biomass burning, biogenic, lightning, aircraft and surface anthropogenic sources. All tracers
10 were run from July 1 through August 15, plus a 10-day spin-up time. The average column NO_x
11 values for each tracer above 6 km are shown in Figure 10. The plot includes both a 10-day
12 passive NO_x tracer which is useful for seeing where the NO_x oxidation products and resulting
13 ozone are transported, and a NO_x tracer with a two-day e-folding lifetime which simulates the
14 decay of NO_x in the upper troposphere and shows where the NO_x primarily exists in the upper
15 troposphere. For both the 10-day passive tracer and 2-day lifetime tracer it is clear that lightning
16 NO_x emissions dominate above eastern North America, followed by anthropogenic surface
17 emissions, with aircraft, biogenic and biomass burning emissions making only small
18 contributions. The 2-day lifetime lightning NO_x maximum is located across northern Mexico, the
19 Gulf of Mexico and the westernmost North Atlantic Ocean. Houston has the greatest column
20 lightning NO_x tracer values while Trinidad Head has the lowest. This distribution is largely the
21 result of: 1) the dominance of lightning activity across the north coast of the Gulf of Mexico; and
22 2) enhanced lightning across the mountainous regions of northern Mexico and southwestern USA
23 associated with the July-August North American monsoon. Much of the lightning NO_x becomes
24 trapped in the upper troposphere above the Gulf of Mexico as it recirculates in the upper
25 tropospheric anticyclone [Li *et al.*, 2005] that is fed by the North American Monsoon. The
26 recirculation is evident in Figure 10 showing the 10-day passive lightning NO_x tracer maximum

1 above the Gulf of Mexico. The recirculation is clearly illustrated in the auxiliary animation of the
2 lightning NO_x tracer. The lightning NO_x tracer is most persistent above the Gulf of Mexico the
3 south-central United States and Mexico. In contrast the lightning NO_x tracer shows a more
4 episodic influence over the rest of east-central North America due to mesoscale convective
5 complexes racing across the Great Plains and weak cold fronts channeling the tracer up the east
6 coast and out into the North Atlantic Ocean.

7 As will be shown in the next section the NO_x in the upper troposphere can produce ozone
8 above southern North America for up to 10 days due to the recirculation of the air above the
9 southern USA. Therefore the total 10-day passive NO_x tracer should roughly correlate with
10 ozone above North America if the upper tropospheric ozone enhancement is driven by in situ
11 ozone production. Figure 11 shows median tropospheric residual ozone above all 15 ozone
12 monitoring sites averaged above 6 km vs. the average 10-day total NO_x tracer above 6 km. We
13 see that ozone does increase with the total NO_x tracer, with the data falling along a straight line
14 ($r^2=0.74$). Houston is located on the far right, with the three upwind sites on the far left. This
15 straight-line correlation is only a qualitative illustration of the relationship between the
16 tropospheric residual ozone and the total NO_x tracer in the upper troposphere, a relationship that
17 is not expected to be strictly linear due to the fact that ozone production efficiency varies with
18 NO_x, CO, CH₄, non-methane hydrocarbons and water vapor mixing ratios as well as sunlight.

19 If we sum up all of the 2-day lifetime NO_x tracer above the east-central region of North
20 America that encompasses the 12 eastern sites we find that lightning NO_x accounts for 80% of the
21 total (84% above Houston only). However in this comparison the quantity of NO_x tracer from
22 surface emissions is greatly over-estimated because we have assumed a 2-day NO_x lifetime which
23 is appropriate for the upper troposphere but not for NO_x emitted into the continental boundary
24 layer where the NO_x lifetime is much shorter. *Li et al.* [2004] estimate that at least 80% of
25 surface NO_x emissions never make it out of the continental boundary layer as they are oxidized in
26 the CBL and removed via wet and dry deposition. If we apply this 80% reduction to the surface

1 anthropogenic and biogenic NO_x emissions (but not to the biomass burning emissions as we
2 assume all of the NO_x is rapidly lofted from the boundary layer due to the heat from the fires) we
3 estimate that lightning NO_x is 95% (96%) of the total NO_x above east-central North America
4 (Houston). The lightning NO_x emission rate that we selected for this study is 6.4 kg N flash⁻¹.
5 This value is towards the higher end of widely varying estimates, which can be as low as 1.3 kg N
6 flash⁻¹ [Beirle *et al.*, 2006]. Even if we reduce our lightning NO_x emissions by a factor of 5 we
7 find that lightning NO_x still accounts for 78% (83%) of the total above east-central North
8 America (Houston). In a separate GEOS-CHEM model study of the North American reactive
9 nitrogen budget during the ICARTT study period *Hudman et al.* [2006] also conclude that
10 lightning is the primary source of NO_x in the upper troposphere above mid-latitude North
11 America.

12 **4. Discussion**

13 In section 3.2 we were conservative and estimated that at least 14 ppbv of the 16 ppbv
14 tropospheric residual ozone enhancement above eastern North America, or 88%, must be due to
15 in situ ozone production in the free troposphere. In Section 3.4 we estimated that at least 78% of
16 the NO_x in the upper troposphere above eastern North America must be due to lightning
17 emissions. Therefore, assuming NO_x from all sources produces ozone with the same efficiency, at
18 least 69% (and up to 84%) of the total ozone enhancement above eastern North America is due to
19 in situ production from lightning NO_x. But can these ozone enhancements really be produced
20 from the estimated NO_x in the upper troposphere, especially above Houston where the ozone
21 enhancement is 25 ppb and the air is not heavily polluted? To answer this question we conducted
22 a box modeling study of ozone production above Houston from lightning NO_x emissions.

23 We began by retrieving the FLEXPART lightning NO_x tracer values along the NASA
24 DC-8 flight tracks over the continental USA during ICARTT and applying an e-folding lifetime
25 to make the modeled values match the median NO_x profile measured by the DC-8. Figure 12
26 shows the results when lifetimes of 1, 2 and 4 days are used. The 2-day lifetime produces the

1 best fit between the modeled and measured median profiles above 6 km, although the 90th
2 percentile of the modeled lightning NO_x is about a factor of 4 too high. The over-estimate at the
3 high end could be due to the DC-8 not intercepting the most concentrated plumes of lightning
4 NO_x. While the DC8 NO_x measurements reached as high as 5 ppbv, other studies have reported
5 NO measurements as high as 9.5, 19 and 25 ppbv in thunderstorm anvils above Florida [*Ridley et*
6 *al.*, 2004], Colorado [*Stith et al.*, 1999] and Germany [*Huntrieser et al.*, 2002], respectively. This
7 2-day lifetime agrees with box model analyses of upper tropospheric NO_x lifetime based on the
8 NASA DC-8 trace gas measurements during ICARTT [*Olson et al.*, 2005]; it also agrees with the
9 NO_x lifetime calculated by *Bertram et al.* [2006] at 10 km, although their NO_x lifetime at 12 km
10 is longer and fresh NO_x injections require 6 days to achieve steady-state mixing ratios. To
11 account for the possibility that our lightning NO_x emission rate of 6.4 kg N flash⁻¹ is too high we
12 conducted a second box model study using an emission rate of 3.2 kg N flash⁻¹. This lower
13 emission rate requires a NO_x lifetime in the upper troposphere of 5 days to force the NO_x tracer to
14 match the DC8 NO_x measurements. This 5-day lifetime falls in the range of values determined by
15 *Jaeglé et al.* [1998] for April-May conditions above the USA, and may be more appropriate given
16 that both the NASA Langley photochemical box model and the model used by *Bertram et al.*
17 [2006] produced greater OH mixing ratios than those observed by the DC-8, which means the
18 actual NO_x lifetime in the upper troposphere could be longer than 2 days.

19 Next, for the times when we had ozone measurements from the IONS and MOZAIC
20 profiles in the upper troposphere, we calculated the net ozone production upwind of Houston over
21 a 10 day-period. This was based on the upwind distribution of FLEXPART NO_x between 9 and
22 12 km with a 2-day lifetime and median upper tropospheric trace gas mixing ratios for relatively
23 clean conditions during INTEX. These clean conditions were based on DC-8 observations in the
24 upper troposphere when CO mixing ratios were less than 100 ppbv, and were chosen to match the
25 MOZAIC CO measurements above east Texas. Calculations were performed using the NASA
26 Langley photochemical box model to provide diurnal-average estimates of net ozone production

1 over each of the 10 days. The most recent description of the model can be found in *Olson et al.*
2 [2006]. Based on these calculations and using a lightning NO_x emission rate of 6.4 kg N flash⁻¹, a
3 net increase in ozone of 29 ppbv could be achieved over the 10 days, accounting for an upper
4 tropospheric ozone lifetime of approximately 90 days. When we removed the relatively small
5 concentrations of reactive non-methane hydrocarbons the net ozone production was 27 ppbv,
6 indicating that large quantities of ozone can be produced even in the absence of fresh
7 anthropogenic emissions. Under these conditions the ozone production is primarily the result of
8 reactions between relatively high NO_x mixing ratios and background mixing ratios of CO and
9 CH₄.

10 When we applied a lightning NO_x emission rate of 3.2 kg N flash⁻¹, the model still
11 produced a net ozone increase of 27 ppbv. This result should not be surprising since the largest
12 changes in the NO_x distribution occurred for the very high NO_x levels (exceeding several ppbv).
13 At ppbv levels, NO_x becomes the dominant sink for the peroxy radicals that facilitate ozone
14 production, thus further increases in NO_x lead to much less efficient production. Instead, most of
15 the ozone increase is associated with the more efficient production in air parcels containing
16 several hundred pptv of NO_x which are abundant in both NO_x distributions. When considering
17 the NO_x distribution observed by the DC-8 which lacked the extremely high values (see Figure
18 12b), the average calculated ozone net production rate is approximately 4 ppbv/day. This
19 production rate could result in an additional 25 ppbv of ozone in about 6-7 days if the NO_x
20 distribution can be sustained. From this analysis we conclude that the upper troposphere above
21 the southern USA contains sufficient lightning NO_x to produce a median ozone enhancement of
22 24 ppbv through oxidation reactions of relatively enhanced NO and background mixing ratios of
23 CH₄ and CO alone. Similar conclusions were reached by *Moxim and Levy* [2000] whose
24 chemical transport model simulation indicated that lightning NO_x in conjunction with CO/CH₄
25 chemistry dominated ozone production in the region of the upper tropospheric ozone
26 enhancement above the tropical South Atlantic Ocean.

1 **5. Conclusions**

2 This study assembled the most comprehensive set of ozone measurements ever collected
3 in the free troposphere above mid-latitude North America during a single season. By focusing on
4 measurements taken only in the troposphere and by calculating and subtracting the influence from
5 aged stratospheric intrusions (up to 20 days old) we produced a dataset of tropospheric residual
6 ozone values across the study region. On average the upper troposphere above mid-latitude
7 eastern North America contained 15 ppbv more tropospheric residual ozone than the more
8 polluted layer between the surface and 2 km above sea level (Figure 3c). Furthermore the upper
9 troposphere above mid-latitude eastern North America contained 16 ppbv more tropospheric
10 residual ozone than the upper troposphere above 3 upwind sites, with the greatest enhancement
11 above Houston at 24 ppbv (Figure 5d).

12 Overall, we estimate that 69-84% (11-13 ppbv) of the 16 ppbv ozone enhancement above
13 eastern North America is due to in situ ozone production from lightning NO_x with the remainder
14 due to transport of ozone from the surface or in situ ozone production from other sources of NO_x .
15 However, the contribution of lightning NO_x to the upper tropospheric ozone maximum above
16 eastern North America should not be considered an entirely natural process because emissions of
17 non-methane hydrocarbons and especially CO and CH_4 are required to produce the ozone, with
18 anthropogenic sources accounting for roughly 60% of CH_4 emissions and 50% of CO emissions
19 [Fiore *et al.*, 2002].

20 This study contains several sources of uncertainty, greatest of which are the lightning
21 NO_x emission rate and the lifetime of NO_x in the upper troposphere, and we have been careful to
22 take the variability of these values into account. We have provided some broad estimates of the
23 lightning NO_x contribution to the widespread upper tropospheric ozone enhancement across
24 eastern North America, and additional chemical transport model studies and measurements are
25 required to refine the quantification of the contribution of lightning NO_x to the upper tropospheric
26 ozone enhancement for the individual measurement stations. However some confirmation of our

1 results is provided by a recent study that showed great foresight into the existence of the upper
2 tropospheric ozone maximum above Texas. *Li et al.* [2005] used a global scale chemical
3 transport model to simulate ozone production above North America for the summer of 2000.
4 They predicted that an ozone maximum would be present in the upper troposphere above the
5 south-central USA as a result of convective lofting of surface ozone, and in situ production by
6 anthropogenic NO_x, lightning NO_x, and formaldehyde produced from surface isoprene emissions.
7 Long residence times in the upper troposphere due to the semi-permanent summertime
8 anticyclone would allow for ozone production over several days. Ozone measurements were
9 limited for the study period and only 6 profiles above Huntsville were available to validate the
10 simulation. Interestingly, the authors found that they had to increase the model-generated
11 lightning NO_x by a factor of 4 above the standard simulation to make the model match the
12 ozonesonde measurements.

13 While this study has revealed an upper tropospheric ozone maximum above Houston we
14 only know that its production begins somewhere east of the west coast and somewhere north of
15 Caracas, Venezuela. Additional ozone profiles are required in western North America and south
16 of the USA to identify where the ozone maximum begins. Another key site on the west coast
17 would be the southern coast of British Columbia to determine if Trinidad Head and Table
18 Mountain are truly representative of air flowing into western North America. Profiles in central
19 Mexico, and at the New Mexico/Mexico border would indicate the amount of ozone flowing into
20 the southern USA with the North American monsoon, while additional profiles in Colorado and
21 Saskatchewan would reveal the northerly extent of this influence. Finally, profiles are needed
22 from the eastern edge of the Caribbean Sea. This location would measure the background ozone
23 that flows from the tropical North Atlantic Ocean into the Gulf of Mexico and on to the southern
24 USA via the North American monsoon flow, while being positioned upwind of the major North
25 American lightning region.

1 **Acknowledgements**

2 The authors gratefully acknowledge the strong support of the MOZAIC program by the European
3 Communities, EADS, Airbus and the airlines (Lufthansa, Austrian, Air France) who have carried
4 the MOZAIC equipment free of charge since 1994. NLDN and LRLDN data were collected by
5 Vaisala-Thunderstorm and supplied to us by the Global Hydrology Resource Center (GHRC) at
6 NASA Marshall Space Flight Center (MSFC). The LIS/OTD 2.5 degree low-resolution lightning
7 climatologies (v0.1 gridded satellite data) are preliminary datasets produced by the NASA
8 LIS/OTD Science Team (Principal Investigator, H. J. Christian, NASA/MSFC) available from
9 GHRC (<http://ghrc.msfc.nasa.gov>). GPCP precipitation plots were made available by NASA
10 Goddard Space Flight Center at <http://precip.gsfc.nasa.gov/>. EDGAR (<http://www.mnp.nl/edgar>)
11 is a product of the National Institute for Public Health and the Netherlands Organisation for
12 Applied Scientific Research, and is part of the Global Emissions Inventory Activity of
13 IGBP/IGAC. We thank Stuart McKeen and Greg Frost at the University of Colorado/NOAA
14 ESRL for making the North American NO_x emission inventory available to us; Dennis Boccippio
15 at NASA for providing the gridded IC:CG ratios; and Don Blake at University of California,
16 Irvine for providing the i-pentane data. Finally we thank two anonymous referees, and Rynda
17 Hudman, Harvard University, and Heidi Huntrieser, Deutsches Zentrum Für Luft- und
18 Raumfahrt, for their helpful comments.

1 **6. References**

- 2 Beirle, S., N. Spichtinger, A. Stohl, K. Cummins, T. Turner, D. Boccippio, O. R. Cooper, M.
3 Wenig, M. Grzegorski, U. Platt and T. Wagner, Estimating the NO_x produced by
4 lightning from GOME data: A case study in the Gulf of Mexico, *Atmos Chem Phys.*, in-
5 press, 2006.
- 6 Bertram, T.H., A. Perring, P. Wooldridge, R.C. Cohen, J. Dibb, E. Scheuer, J. Crouse, P.
7 Wennberg, S. Vay, S. Kim, G. Huey, J. Walega, A. Fried, M. Porter, H. Fuelberg, B.
8 Heikes, G. Sachse, M. Avery and A. Clarke, Convection and the Age of Air in the Upper
9 Troposphere, manuscript in preparation for submission to *J. Geophys. Res.*, 2006.
- 10 Boccippio, D. J., K. L. Cummins, H. J. Christian and S. J. Goodman, Combined satellite- and
11 surface-based estimation of the intracloud-cloud-to-ground lightning ratio over the
12 continental United States, *Mon. Wea. Rev.*, 129, 108-122, 2001.
- 13 Cleary, P. A., P.J. Wooldridge, R.C. Cohen, (2002), Laser-induced fluorescence detection of
14 atmospheric NO₂ with a commercial diode laser and a supersonic expansion, *Applied*
15 *Optics*, 41, 6950-6956.
- 16 Christian, H. J., R. J. Blakeslee, D. J. Boccippio, W. L. Boeck, D. E. Buechler, K. T. Driscoll, S.
17 J. Goodman, J. M. Hall, W. J. Koshak, D. M. Mach, and M. F. Stewart, Global
18 frequency and distribution of lightning as observed from space by the Optical Transient
19 Detector, *J. Geophys. Res.*, 108(D1), 4005, doi:10.1029/2002JD002347, 2003
- 20 Colman, J. J., A. L. Swanson, S. Meinardi, B. C. Sive, D. R. Blake, F. S. Rowland, Description of
21 the Analysis of a Wide Range of Volatile Organic Compounds in Whole Air Samples
22 Collected during PEM-Tropics A and B, *Anal. Chem.* 73(15), 3723-3731,
23 doi:10.1021/ac010027g, 2001.
- 24 Cooper, O. R., A. Stohl, S. Eckhardt, D. D. Parrish, S. J. Oltmans, B. J. Johnson, P. Nedelec, F. J.
25 Schmidlin, M. J. Newchurch, Y. Kono and K. Kita, A springtime comparison of

1 tropospheric ozone and transport pathways on the east and west coasts of the United
2 States, *J. Geophys. Res.*, *110*, D05S90, doi:10.1029/2004JD005183, 2005a.

3 Cooper O. R., et al. (2005b), Direct transport of midlatitude stratospheric ozone into the lower
4 troposphere and marine boundary layer of the tropical Pacific Ocean, *J. Geophys. Res.*,
5 *110*, D23310, doi:10.1029/2005JD005783.

6 DeCaria, A. J., K. E. Pickering, G. L. Stenchikov, and L. E. Ott (2005), Lightning-generated NO_x
7 and its impact on tropospheric ozone production: A three-dimensional modeling study of
8 a Stratosphere-Troposphere Experiment: Radiation, Aerosols and Ozone (STRAO-A)
9 thunderstorm, *J. Geophys. Res.*, *110*, D14303, doi:10.1029/2004JD005556.

10 Emanuel, K.A., and M. Živković-Rothman, Development and evaluation of a convection scheme
11 for use in climate models, *J. Atmos. Sci.*, *56*, 1766-1782, 1999.

12 Fishman, J., and A. E. Balok, Calculation of daily tropospheric ozone residuals using TOMS and
13 empirically improved SBUV measurements: Application to an ozone pollution episode
14 over the eastern United States, *J. Geophys. Res.*, *104*, 30,319-30,340, 1999.

15 Fiore A. M., D. J. Jacob, J. A. Logan, Long-term trends in ground level ozone over the
16 contiguous United States, 1980-1995, *J. Geophys. Res.*, *103*, 1471-1480, 1998.

17 Fiore, A. M., D. J. Jacob, B. D. Field, D. G. Streets, S. D. Fernandes, C. Jang, Linking ozone
18 pollution and climate change: The case for controlling methane, *Geophys. Res. Lett.*, *29*,
19 Art. No. 1919, 2002

20 Forster, C., A. Stohl, P. James and V. Thouret, The residence times of aircraft emissions in the
21 stratosphere using a mean emission inventory and emissions from actual flight tracks, *J.*
22 *Geophys. Res.*, *108*(D12), 8524, doi:10.1029/2002JD002515, 2003.

23 Forster, C., A. Stohl, and P. Seibert (2006): Parameterization of convective transport in a
24 Lagrangian particle dispersion model and its evaluation, *J. Appl. Met. Clim.*, in-review.

25 Frost, G. J., S. A. McKeen, M. Trainer, T. B. Ryerson, J. S. Holloway, D. T. Sueper, T. Fortin, D.
26 D. Parrish, F. C. Fehsenfeld, S. E. Peckham, G. A. Grell, D. Kowal, J. Cartwright, N.

1 Auerbach, and T. Habermann, Effects of Changing Power Plant NO_x Emissions on
2 Ozone in the Eastern United States, *J. Geophys. Res.*, submitted, 2005.

3 Grogan, M. J., Report on the 2002-2003 US NLDN system-wide upgrade, Vaisala Thunderstorm,
4 Tuscon, 2004.

5 [http://www.vaisala.com/businessareas/measurementsystems/thunderstorm/knowledgecent](http://www.vaisala.com/businessareas/measurementsystems/thunderstorm/knowledgecenter/aboutnldn)
6 [er/aboutnldn](http://www.vaisala.com/businessareas/measurementsystems/thunderstorm/knowledgecenter/aboutnldn)

7 Hudman, R.C., D.J. Jacob, S. Turquety, L.T. Murray, S. Wu, M. Avery, T.H. Bertram, E.
8 Browell, W. Brune, R.C. Cohen, J.E. Dibb, F.M. Flocke, A. Gilliland, J. Holloway, A.
9 Neuman, X. Ren, T.B. Ryerson, G.W. Sachse, H.B. Singh, P.J. Wooldridge, A multi-
10 platform analysis of the North American reactive nitrogen budget during the ICARTT
11 summer intensive, *manuscript in preparation*, 2006.

12 Huntrieser, H., H. Schlager, C. Feigl, H. Höller, Transport and production of NO_x in electrified
13 thunderstorms: Survey of previous studies and new observations at midlatitudes, *J.*
14 *Geophys. Res.*, 103(D21), 28247-28264, 10.1029/98JD02353, 1998.

15 Huntrieser H., C. Feigl, H. Schlager, F. Schröder, C. Gerbig, P. van Velthoven, F. Flatøy, C.
16 Théry, A. Petzold, H. Höller, and U. Schumann, Airborne measurements of NO_x, tracer
17 species, and small particles during the European Lightning Nitrogen Oxides Experiment,
18 *J. Geophys. Res.*, 107, doi:10.1029/2000JD000209, 2002.

19 IPCC, 2001: Climate Change 2001: The Scientific Basis. Contribution of Working Group I to the
20 Third Assessment Report of the Intergovernmental Panel on Climate Change [Houghton,
21 J. T., Y. Ding, D. J. Griggs, M. Noguer, P. J. van der Linden, X. Dai, K. Maskell, and C.
22 A. Johnson (eds.)]. Cambridge University Press, Cambridge, United Kingdom and New
23 York, NY, USA, 881 pp.

24 Jaeglé, L., D. J. Jacob, Y. Wang, A. J. Weinheimer, B. A. Ridley, T. L. Campos, G. W. Sachse,
25 and D. E. Hagen, Sources and chemistry of NO_x in the upper troposphere over the United
26 States, *Geophys. Res. Lett.*, 25, 1705-1708, 1998.

1 Li, Q., D. J. Jacob, I. Bey, P. I. Palmer, B. N. Duncan, B. D. Field, R. V. Martin, A. M. Fiore, R.
2 M. Yantosca, D. D. Parrish, P. G. Simmonds, and S. J. Oltmans, Transatlantic transport
3 of pollution and its effects on surface ozone in Europe and North America, *J. Geophys.*
4 *Res.*, 107(D13), 4166, doi:10.1029/2001JD001422, 2002.

5 Li, G. D. J. Jacob, J. W. Munger, R. M. Yantosca and D. D. Parrish, Export of NO_y from the
6 North American boundary layer: Reconciling aircraft observations and global model
7 budgets, *J. Geophys. Res.*, 109, D02313, doi:10.1029/2003JD004086, 2004.

8 Li, Q., D. J. Jacob, R. Park, Y. Wang, C. L. Heald, R. Hudman, R. M. Yantosca, R. V. Martin,
9 and M. Evans, North American pollution outflow and the trapping of convectively lifted
10 pollution by upper-level anticyclone, *J. Geophys. Res.*, 110, D10301,
11 doi:10.1029/2004JD005039, 2005.

12 McDermid, I. S., G. Beyerle, D. A. Haner, and T. Leblanc, Redesign and improved performance
13 of the tropospheric ozone lidar at the Jet Propulsion Laboratory Table Mountain Facility,
14 *Applied Optics*, 41, 7550-7555, 2002.

15 Morris G. A., S. Hersey, A. M. Thompson, S. Pawson, J. E. Nielsen, P. R. Colarco, W. W.
16 McMillan, A. Stohl, S. Turquety, J. Warner, B. J. Johnson, T. L. Kucsera, D. E. Larko, S.
17 J. Oltmans, and J. C. Witte, Alaskan and Canadian forest fires exacerbate ozone pollution
18 over Houston, Texas, on 19 and 20 July 2004, submitted to *J. Geophys. Res.*, 2006.

19 Mortlock, A. M., and R. Van Alstyne, Military, Charter, Unreported Domestic Traffic and
20 General Aviation: 1976, 1984, 1992, and 2015 Emission Scenarios, NASA CR- 1998-
21 207639, 1998. Available at
22 http://ntrs.nasa.gov/archive/nasa/casi.ntrs.nasa.gov/19980047346_1998120131.pdf

23 Moxim, W. J., and H Levy II, A model analysis of the tropical South Atlantic Ocean tropospheric
24 ozone maximum: The interaction of transport and chemistry, *J. Geophys. Res.*, 105,
25 17,393-17,415, 2000.

1 Nedelec, P., J.-P. Cammas, V. Thouret, G. Athier, J.-M. Cousin, C. Legrand, C. Abonnel, F.
2 Lecoecur, G. Cayez, and C. Marizy, An improved infrared carbon monoxide analyser for
3 routine measurements aboard commercial Airbus aircraft: technical validation and first
4 scientific results of the MOZAIC III programme, *Atmos. Chem. Phys.*, 3, 1551-1564,
5 2003.

6 Newchurch, M. J., M. A. Ayoub, S. Oltmans, B. Johnson, and F. J. Schmidlin, Vertical
7 distribution of ozone at four sites in the United States, *J. Geophys. Res.*, 108(D1), 4031,
8 doi:10.1029/2002JD002059, 2003.

9 Olivier, J.G.J. and J.J.M. Berdowski (2001) Global emissions sources and sinks. In: Berdowski,
10 J., Guicherit, R. and B.J. Heij (eds.) "The Climate System", pp. 33-78. A.A. Balkema
11 Publishers/Swets & Zeitlinger Publishers, Lisse, The Netherlands. ISBN 90 5809 255 0.

12 Olson, J. R., J. Crawford, G. Chen, M. Pippin, W. Brune, X. Ren, R. Cohen, A. Fried, B. Heikes,
13 D. O'Sullivan, G. Huey, P. Wennberg, and J. Crouse (2005), An examination of
14 photochemical theory based on INTEX-NA observations, paper presented at AGU Fall
15 Meeting, San Francisco, Calif., 5-9 December.

16 Olson, J. R., J. H. Crawford, G. Chen, W. H. Brune, I. C. Faloona, D. Tan, H. Harder, and M.
17 Martinez, A reevaluation of airborne HO_x observations from NASA field campaigns, *J.*
18 *Geophys. Res.*, *in-press*, 2006.

19 Orville, R. E., G. R. Huffines, W. R. Burrows, R. L. Holle and K. L. Cummins, The North
20 American Lightning Detection Network (NALDN) – First Results: 1998-2000, *Monthly*
21 *Weather Review*, 130, 2098-2109. 2002.

22 Pickering, K. E., Y. Wang, W.-K. Tao, C. Price, J.-F. Müller, Vertical distributions of lightning
23 NO_x for use in regional and global chemical transport models, *J. Geophys. Res.*,
24 103(D23), 31203-31216, 10.1029/98JD02651, 1998.

1 Pierce, T., C. Geron, L. Bender, R. Dennis, G. Tonneson, and A. Guenther, Influence of increased
2 isoprene emissions on regional ozone modeling, *J. Geophys. Res.*, *103*, 25,611-25,629,
3 1998.

4 Ridley, B., L. Ott, K. Pickering, L. Emmons, D. Montzka, A. Weinheimer, D. Knapp, F. Grahek,
5 L. Li, G. Heymsfield, M. McGill, P. Kucera, M. J. Mahoney, D. Baumgardner, M.
6 Schultz, and G. Brasseur, (2004), Florida thunderstorms: A faucet of reactive nitrogen to
7 the upper troposphere, *J. Geophys. Res.*, *109*, D17305, doi:10.1029/2004JD004769.

8 Ridley, B. A., K. E. Pickering, and J. E. Dye, Comments on the parameterization of lightning-
9 produced NO in global chemistry-transport models, *Atmos. Environ.*, *39*, 6184-6187,
10 2005.

11 Stith, J., J. Dye, B. Ridley, P. Laroche, E. Defer, K. Baumann, G. Hübler, R. Zerr, M.
12 Venticinque, NO signatures from lightning flashes, *J. Geophys. Res.*, *104*, 16081-16090,
13 10.1029/1999JD900174, 1999.

14 Stohl, A., M. Hittenberger, and G. Wotawa, Validation of the Lagrangian particle dispersion
15 model FLEXPART against large scale tracer experiment data, *Atmos. Environ.*, *32*, 4245-
16 4264, 1998.

17 Stohl, A., M. Trainer, T. B. Ryerson, J. S. Holloway, and D. D. Parrish, Export of NO_y from the
18 North American boundary layer during 1996 and 1997 North Atlantic Regional
19 Experiments, *J. Geophys. Res.*, *107*(D11), 10.1029/2001JD000519, 2002.

20 Stohl, A., C. Forster, S. Eckhardt, N. Spichtinger, H. Huntrieser, J. Heland, H. Schlager, H.
21 Aufmhoff, F. Arnold and O. Cooper, A backward modeling study of intercontinental
22 pollution transport using aircraft measurements, *J. Geophys. Res.*, *108*(D12), 4370,
23 10.1029/2002JD002862, 2003.

24 Stohl, A., C. Forster, A. Frank, P. Seibert and G. Wotowa, Technical Note: The Lagrangian
25 particle dispersion model FLEXPART version 6.2, *Atmos. Chem. Phys.*, *5*, 2461-2474,
26 2005.

1 Sutkus, D. J., Jr., S. L. Baughcum and D. P. DuBois, Scheduled civil aircraft emission inventories
2 for 1999: Database development and analysis, NASA/CR-2001-211216, Glen Research
3 Center, 2001.

4 Tarasick, D. W., V. E. Fioletov, D. I. Wardle, J. B. Kerr, and J. Davies, Changes in the vertical
5 distribution of ozone over Canada from ozonesondes: 1980–2001, *J. Geophys. Res.*, *110*,
6 D02304, doi:10.1029/2004JD004643, 2005.

7 Thompson, A. M., J. B. Stone, J. C. Witte, R. B. Pierce, R. B. Chatfield, S. J. Oltmans, O. R.
8 Cooper, B. F. Taubman, B. J. Johnson, E. Joseph, T. L. Kucsera, J. T. Merrill, G. A.
9 Morris, S. Hersey, M. J. Newchurch, F. J. Schmidlin, D. W. Tarasick, V. Thouret and J.
10 P. Cammas, IONS-04 (INTEX Ozonesonde Network Study, 2004): Perspective on
11 Summertime UT/LS (Upper Troposphere/Lower Stratosphere) ozone over northeastern
12 North America, *J. Geophys. Res.*, *in-review*, 2006JD007441, 2006.

13 Thornton, J. A., P.J. Wooldridge, R.C. Cohen, (2000), Atmospheric NO₂: In situ laser-induced
14 fluorescence detection at parts per trillion mixing ratios, *Analytical Chemistry*, *72*, 528-
15 539.

16 Thouret, V., A. Marenco, J. A. Logan, P. Nédélec, and C. Grouhel, Comparisons of ozone
17 measurements from the MOZAIC airborne program and the ozone sounding network at
18 eight stations, *J. Geophys. Res.*, *103*, 25,695-25,720, 1998.

19 Turquety, S., D. J. Jacob, J. A. Logan, R. C. Hudman, R. M. Yevich, F. Y. Leung, C. L. Heald, R.
20 M. Yantosca, S. Wu, L. K. Emmons, D. P. Edwards, and G. W. Sachse, Inventory of
21 boreal fire emissions for North America: importance of peat burning and pyro-convective
22 injection, *manuscript in preparation for J. Geophys. Res.*, 2006.

23 Yieinger, J.J., and H. Levy II, Empirical model of global soil-biogenic NO_x emissions, *J.*
24 *Geophys. Res.*, *100*, 11,447-11,464, 1995.

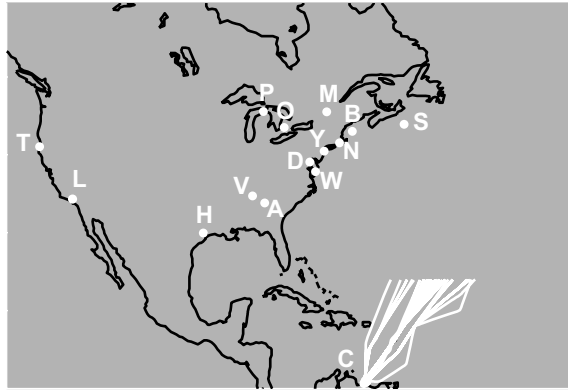


Figure 1. The locations of the fourteen ozone profile sites in 2004: Trinidad Head (T), Table Mtn/MOZAIC (L), Houston (H), Huntsville (V), Atlanta (A), Wallops Island (W), Washington DC (D), New York City (Y), Narragansett (N), research vessel R. H. Brown (B), Sable Island (S), Montreal (M), Ontario (O), Pellston (P). The locations of the tropical portions of the MOZAIC flights to and from Caracas (C) during 1999-2004 are also shown.

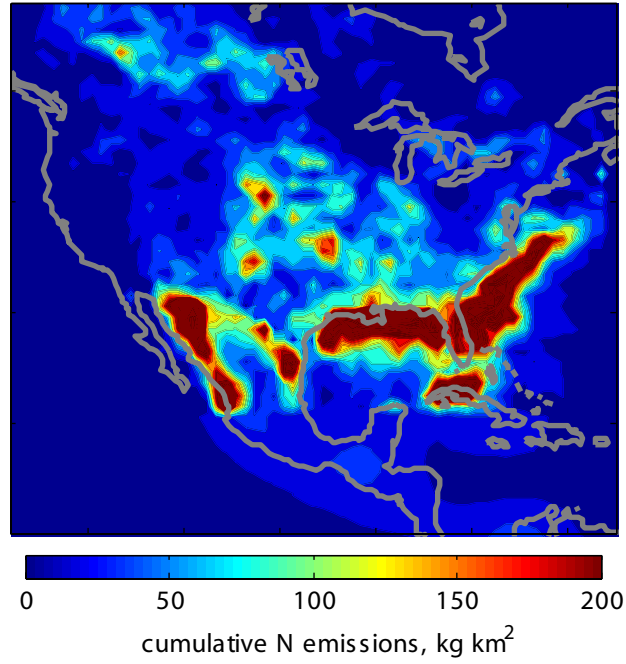


Figure 2. Cumulative lightning N emissions from CG and IC flashes between June 21 and August 15, 2004.

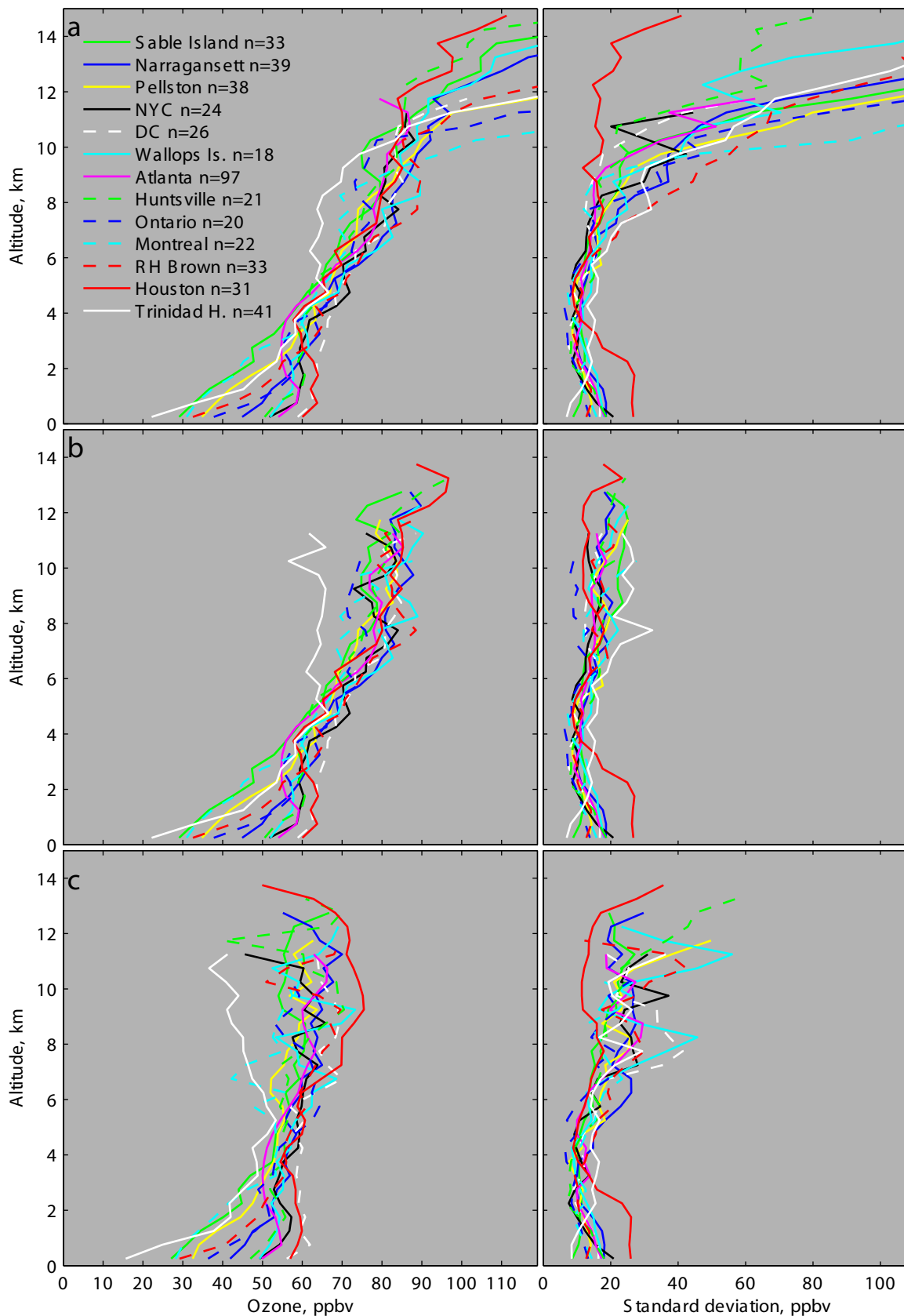


Figure 3. a) Median ozone profiles at all thirteen sites for July 1 - August 15, 2004, reported in 500 m layers with the sample size indicated by n, and the corresponding standard deviations to the right. b) Median ozone profiles for measurements taken only within the troposphere ($PV < 1.0$), and the corresponding standard deviations to the right. c) Median ozone profiles after the estimated stratospheric influence from the past 20 days has been removed, with standard deviations to the right.

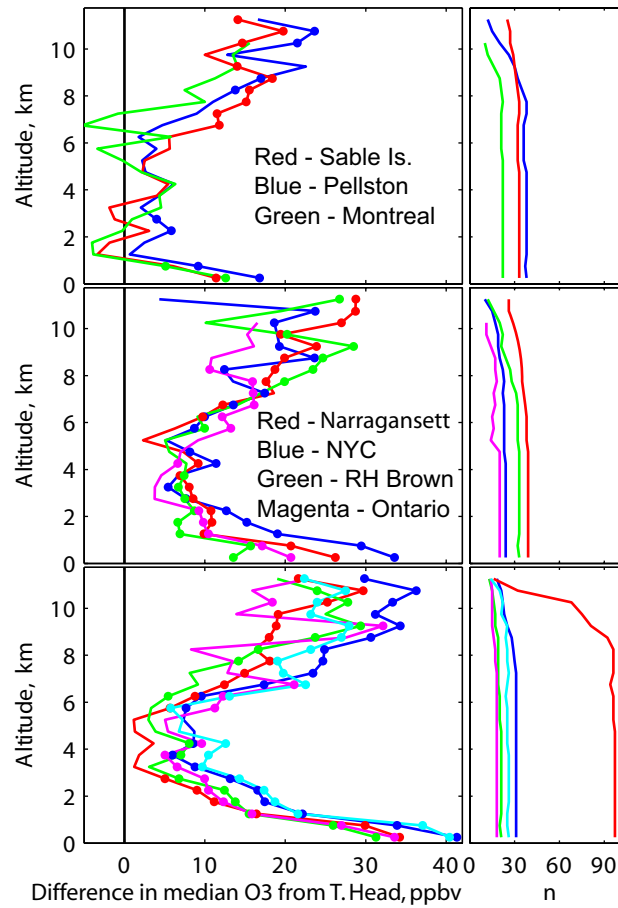


Figure 4. Difference in median O₃ values between sites in eastern North America and Trinidad Head. Solid circles on the profiles indicate the 500 m layers with O₃ distributions that are significantly different from Trinidad Head at the 95% confidence interval. The sites are partitioned into three regions: north of 44° N (top), northeast USA or eastern Canada (middle), and Mid-Atlantic or southern states (bottom): Houston (blue), Atlanta (red), Huntsville (green), Wallops Is. (magenta), Washington DC (cyan). The right hand plots indicate the sample size in each 500 m layer.

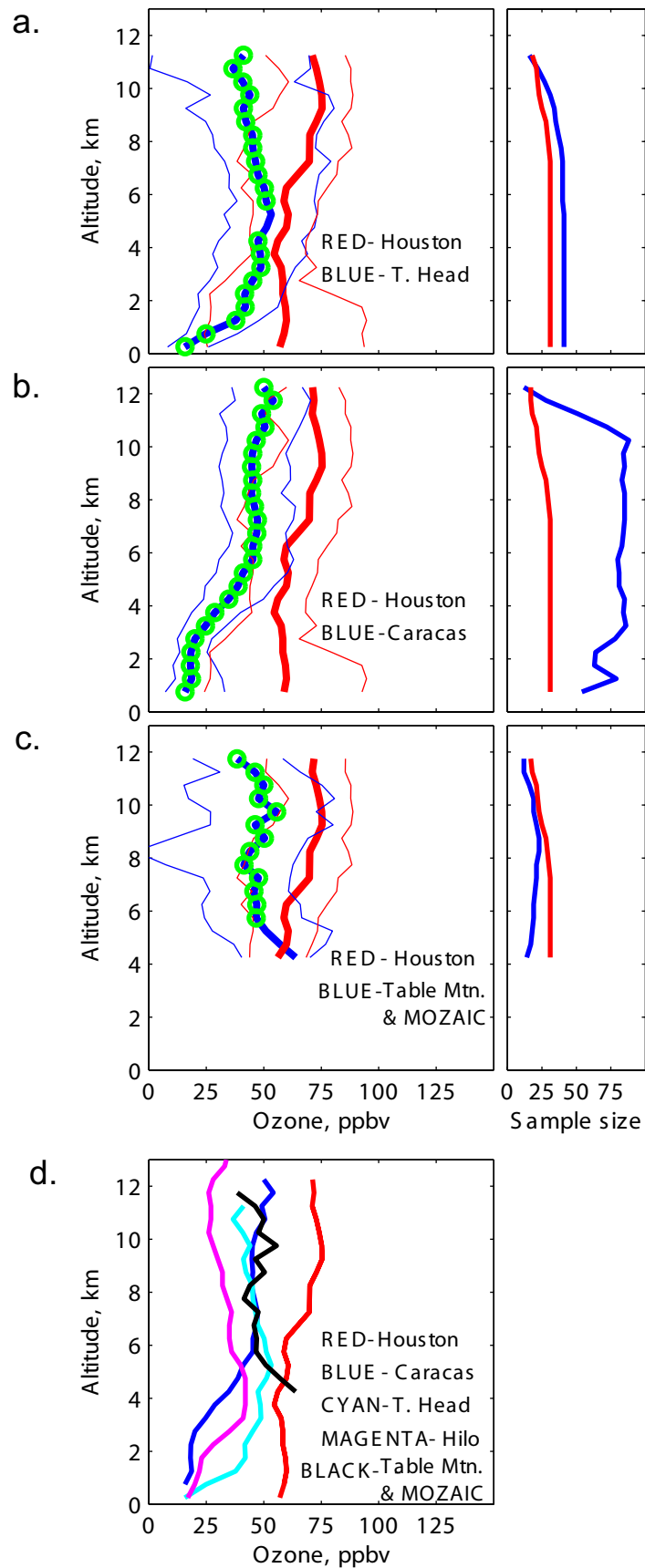


Figure 5. Comparison of ozone distributions between a) Houston and Trinidad Head, b) Houston and Caracas, and c) Houston and Table Mtn/MOZAIC. Shown are median values (thick lines) and 10th and 90th percentiles (thin lines), with green circles indicating those 500 m layers with ozone distributions that are significantly different at the 95% confidence interval. In (d) median ozone values at Houston are compared to the upwind sites of Caracas, Trinidad Head, Table Mountain/MOZAIC and Hilo, Hawaii, which has 62 profiles in July and August from 1999-2005.

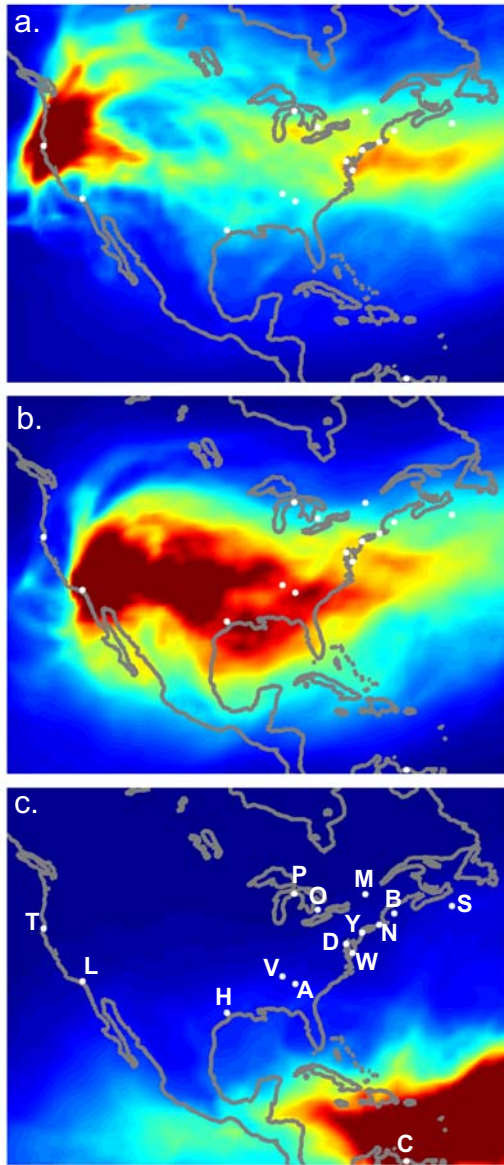


Figure 6. Eleven million trajectory particles were released between 6 km above sea level and the tropopause during the study period from Trinidad Head (a), Los Angeles (b) and the eastern edge of the Caribbean (c) and allowed to advect for 20 days. Shown are the average locations of the trajectories (in arbitrary units) above 6 km. The locations of the ozone profile stations are indicated: Trinidad Head (T), Table Mtn/Los Angeles (L), Houston (H), Huntsville (V), Atlanta (A), Wallops Island (W), Washington DC (D), New York City (Y), Narragansett (N), research vessel R. H. Brown (B), Sable Island (S), Montreal (M), Ontario (O), Pellston (P) and Caracas (C).

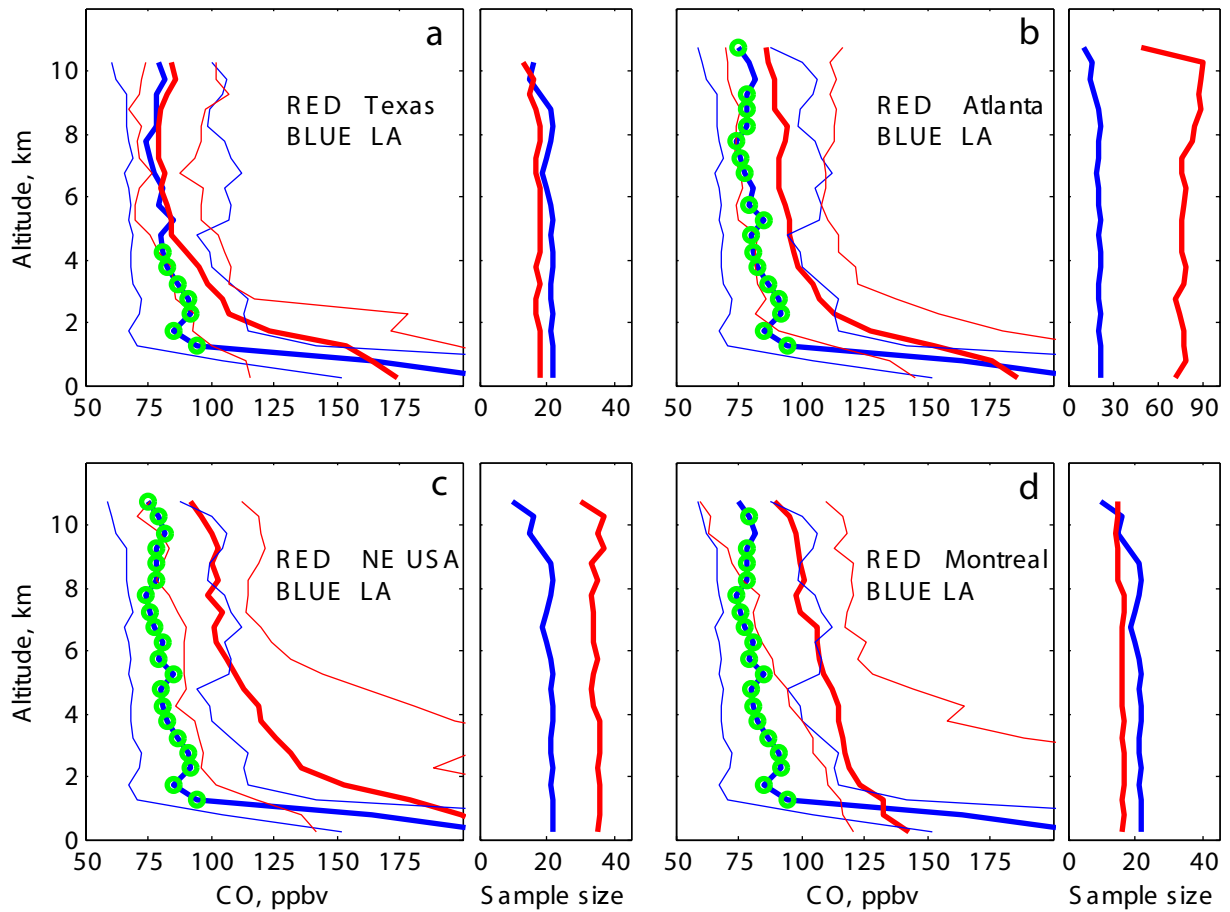


Figure 7. MOZAIC CO distribution above (a) Texas (Houston and Dallas), (b) Atlanta, (c) northeastern USA (New York City and Boston), and (d) Montreal, compared to the median values above Los Angeles during July 1 - August 15, 2004. Shown are median values (thick lines) and the 10th and 90th percentiles (thin lines), with green circles indicating those 500 m layers at the downwind sites that have a CO distribution statistically significant from Los Angeles at the 95% confidence interval. Sample sizes are indicated to the right of each plot.

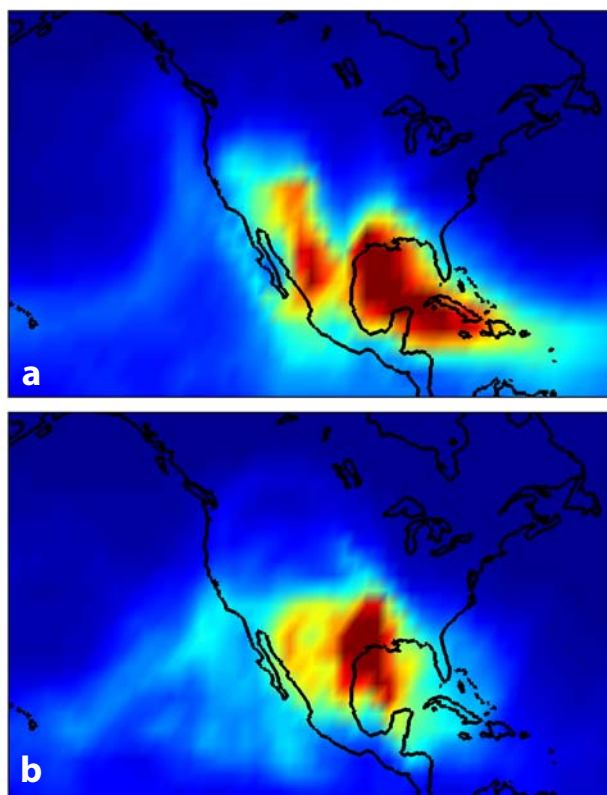


Figure 8. a) 20-day retroplumes were run for each 500 m layer between 6 and 12 km above Houston. The residence times of the particles that passed through the 300 meter layer adjacent to the Earth's surface were tabulated and averaged over all retroplumes. This image depicts the surface locations with the highest incidence of transport to the 6-12 km region above Houston in arbitrary residence time units. b) As in a) but the residence time is tabulated for the atmosphere above 5 km. The arbitrary units in a) had to be increased by a factor of 100 to put them on the same color scale as b). Therefore the quantity of air transported from the regions in a) is small compared to transport from regions in b).

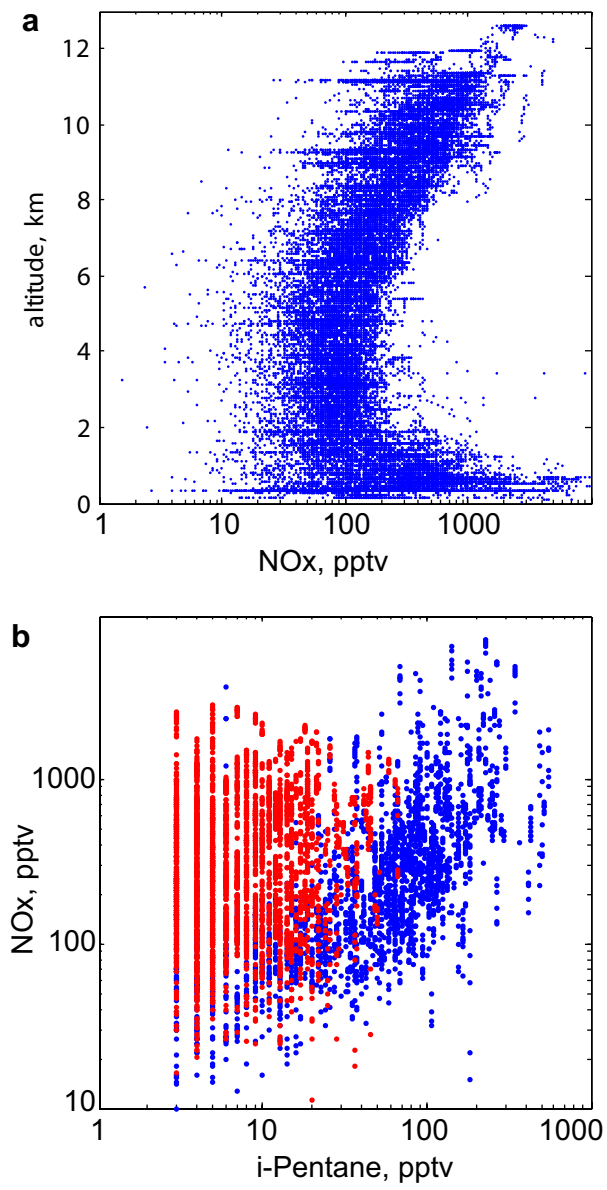


Figure 9. All available 10-second average measurements from the NASA DC8 from all flights between July 1 and August 15, 2004. a) altitude vs. NO_x, b) NO_x vs. i-pentane below 2 km (blue) and above 8 km (red).

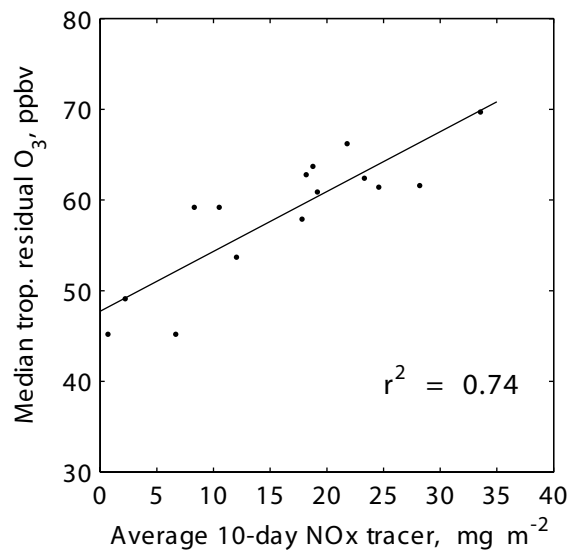


Figure 11. Median tropospheric residual ozone above 6 km (as taken from Figure 3c) vs. the average 10-day total NOx tracer above 6 km (as taken from Figure 10).

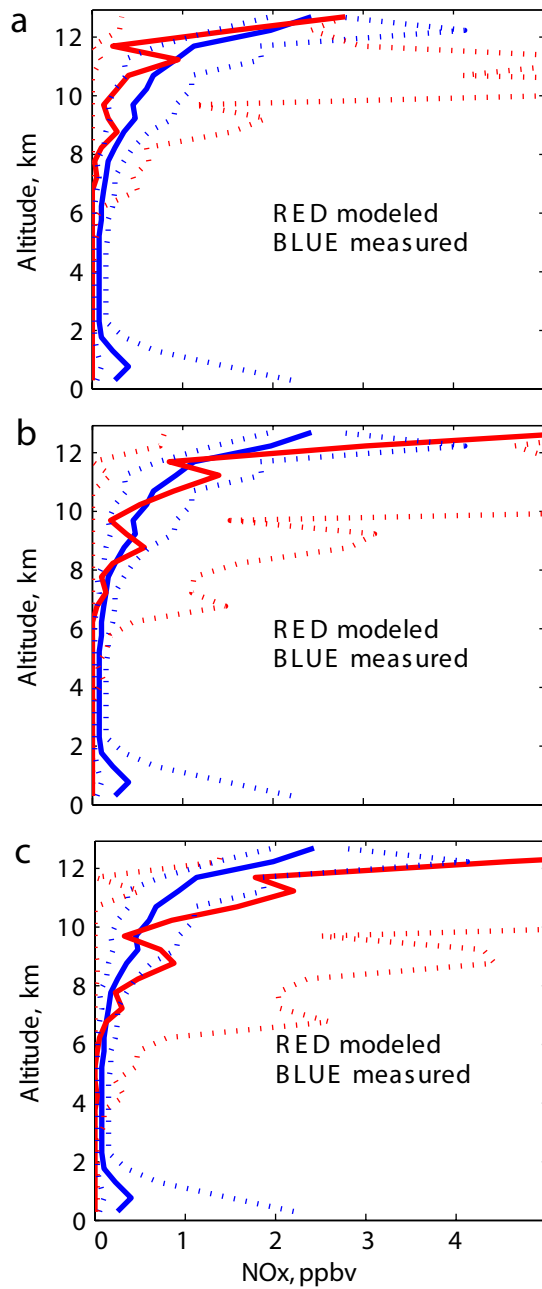


Figure 12. Distributions of measured NO_x (blue) from the DC8 above eastern North America during July 1- August 15, 2004, and the corresponding FLEXPART lightning NO_x tracer values (red). Shown are the median values (solid lines) and the 10th and 90th percentiles (dashed lines) with modeled NO_x lifetimes of (a) 1-day, (b) 2-days, and (c) 4-days.